BILINGUAL PUBLISHING GROUP

Journal of Environmental & Earth Sciences

https://journals.bilpubgroup.com/index.php/jees

ARTICLE

Effect of Scattered Solar Radiation on the Informativeness of Polarization Lidar Studies of High-Level Clouds

Ignatii Samokhvalov, Ilia Bryukhanov, Ivan Akimov, Olesia Kuchinskaia *, Maxim Penzin, Denis Romanov, Evgeny Ni, Ivan Zhivotenyuk

National Research Tomsk State University, Tomsk 634050, Russia

ABSTRACT

During daylight laser polarization sensing of high-level clouds (HLCs), the lidar receiving system generates a signal caused by not only backscattered laser radiation, but also scattered solar radiation, the intensity and polarization of which depends on the Sun's location. If a cloud contains spatially oriented ice particles, then it becomes anisotropic, that is, the coefficients of directional light scattering of such a cloud depend on the Sun's zenith and azimuth angles. In this work, the possibility of using the effect of anisotropic scattering of solar radiation on the predictive ability of machine learning algorithms in solving the problem of predicting the HLC backscattering phase matrix (BSPM) was evaluated. The hypothesis that solar radiation scattered on HLCs has no effect on the BSPM elements of such clouds determined with a polarization lidar was tested. The operation of two algorithms for predicting the BSPM elements is evaluated. To train the first one, meteorological data were used as input parameters; for the second algorithm, the azimuthal and zenith angles of the Sun's position were added to the meteorological parameters. It is shown that there is no significant improvement in the predictive ability of the algorithm.

Keywords: High-Level Clouds (HLCs); Polarization Lidar; Backscattering Phase Matrix (BSPM); Sun's Azimuthal and Zenith Angles; Scattered Solar Radiation; Cloud Microphysics; Machine Learning (ML); Random Forest

*CORRESPONDING AUTHOR:

Olesia Kuchinskaia, National Research Tomsk State University, Tomsk 634050, Russia; Email: OlesyaTSU14@mail.ru

ARTICLE INFO

Received: 18 December 2024 | Revised: 12 January 2025 | Accepted: 20 January 2025 | Published Online: 6 June 2025

DOI: https://doi.org/10.30564/jees.v7i6.8139

CITATION

Samokhvalov, I., Bryukhanov, I., Akimov, I., et al., 2025. Effect of Scattered Solar Radiation on the Informativeness of Polarization Lidar Studies of High-Level Clouds. Journal of Environmental & Earth Sciences. 7(6): 148–156. DOI: https://doi.org/10.30564/jees.v7i6.8139

1. Introduction

The study of atmospheric processes is crucial for understanding environmental change, predicting climate variations, and developing strategies to mitigate the effects of dangerous natural phenomena. To this day, despite significant advances in atmospheric science, many aspects of the atmosphere's behavior remain poorly understood due to its complexity. The process of identifying connections between atmospheric characteristics and external factors affecting its state is a challenging and multidimensional task [1,2]. Lidar (Light Identification, Detection, and Ranging) systems are a powerful tool for remote sensing of aerosol formations in the atmosphere including high-level clouds (HLCs). However, processing and interpreting lidar data often requires complex analysis methods. In this context, it is relevant to consider the use of machine learning (ML) techniques for processing the data of the experiments on remote sensing of natural environment, as well as for solving inverse problems in atmospheric physics, ecology, etc. These methods allow detecting and investigating of interrelationships between various parameters in large volumes of data that would be difficult to identify through classical statistical analysis [3–6].

The solar radiation flux reaching the Earth's surface is formed by a combination of direct and scattered components. Scattered radiation is formed because of the interaction between direct radiation and atmospheric gases (molecular scattering), water droplets in clouds and fog, ice crystals in clouds, and aerosol particles. Most of the solar radiation energy that reaches the Earth's surface is in the short-wavelength spectral region, with wavelengths ranging from approximately 300 to 4,000 nm [7]. The scattered radiation flux depends on the transparency of the atmosphere and is primarily determined by the number of clouds in the sky and their optical and microphysical properties. Aerosol particles in the atmosphere scatter and absorb solar radiation, directly changing the amount of radiation reaching a particular location. In addition, aerosol particles act as condensation nuclei of water vapor contained in the air, and, thereby, accelerating the process of cloud formation [8]. Under clear weather conditions, scattered radiation accounts for approximately 15–20% of the total radiation in warm and cold weather [9].

The relationship between the energy flow of solar radiation entering the Earth's surface and the transparency of the atmosphere is being studied by the world scientific community because a change in the Earth's radiation budget may indicate increased air pollution associated with increasing anthropogenic emissions, which leads to changes in weather in certain regions of the Earth and global climate [10]. For example, in [11], the characteristics of solar radiation in the surface layer of the atmosphere were studied under various air pollution conditions over Nanjing, China. The change in the flow of radiation affects the surface temperature, the processes of evaporation and condensation of water vapor, the water cycle and, in general, the Earth's ecosystem [12]. Cirrus clouds have less effect on the transmission of direct solar radiation compared to other clouds due to their insignificant optical thickness. At the same time, the large horizontal extent of such clouds, which takes values up to a thousand kilometers [13], as well as the presence of horizontally oriented ice particles in HLCs (such clouds are called specular) significantly affect the fluxes of scattered solar radiation.

Existing atmospheric models, including the global model of the European Centre for Medium-Range Weather Forecast (ECMWF), do not take into account the special features of the atmospheric microstructure. Determining the parameters of the microstructure of clouds is a non–trivial task due to the variety of shapes of ice particles in them and the complexity of the mathematical description of their size distributions. As a rule, the concept of an effective radius based on the equality of one of the characteristics of particles and a certain model sphere is used [14]. This simplification allows the Mi theory to be used in calculating the HLC radiation characteristics, but, apparently, it leads to errors in weather and climate forecasts.

The maximum information about the microphysical parameters of the particle ensemble available for obtaining in a light scattering experiment is contained in the scattering phase matrix (SPM) [15]. A lidar allows the SPM to be obtained only for angles close to the direction of 180 degrees, which is called the backscattering matrix (BSPM). The polarization laser sensing method [16], which is based on determining the BSPM, is informative on the shape and orientation of ice particles in HLCs. During laser polarization sensing of such clouds in the daytime, the lidar receiv-

ing system receives not only a lidar signal caused by backscattered laser radiation, but also solar radiation scattered by HLCs, the intensity and polarization of which depends on the Sun's position in the sky. If the cloud contains spatially oriented ice particles, it becomes anisotropic, that is, the coefficients of directional light scattering of such a cloud depend on the Sun's zenith and azimuth angles.

The article employed the machine learning (ML) tools to investigate the correlation between HLC BSPM elements and meteorological conditions[17]. In the present work we evaluate the effect of solar radiation scattered by HLCs on the performance of these algorithms when using them to process data on the laser sensing of clouds in the daytime. The hypothesis of the absence of the effect of scattered UV radiation on the BSPM elements determined with the polarization lidar was tested with appropriate correction of experimentally obtained lidar signals. It was assumed that the intensity of solar radiation scattered by clouds was measured independently. The operation of two algorithms for predicting the BSPM elements was evaluated. To train the first one, meteorological data was used as input parameters; for the second algorithm, the Sun's azimuth and zenith angles were added to the meteorological parameters. It is shown that there is no significant improvement in the predictive power of the algorithm.

2. Materials and Methods

In the present work, the data obtained with the high-altitude matrix polarization leader (HAMPL) developed at the National Research Tomsk State University (NR TSU) were used [18]. It should be noted that the HAMPL database contains the results of experiments performed from 2009 to 2024. To assess the meteorological situation at the altitudes of the examined clouds, data from the ERA5 reanalysis of the European Centre for Medium-Range Weather Forecasts were used. The lidar is located in Tomsk and is oriented vertically in the zenith direction. The HAMPL block diagram is shown in **Figure 1**.

The HAMPL design is equipped with a Nd: YAG laser operating at a wavelength of 532 nm with a pulse energy of up to 400 mJ, and a pulse repetition rate of 10 Hz, which is used as an optical radiation source. A Cassegrain mirror lens with a primary mirror diameter of 0.5 m and a focal length of 5 m is used as a receiving antenna. The lidar receiving system includes the ThorLabs FL532-1 interference filter with a central wavelength of 532 ± 0.6 nm and a half-width of the transmission spectrum of 3 ± 0.6 m. Then the Wollaston prism, which divides received backscattered radiation into two orthogonally polarized beams, is mounted. These radiation beams are registered with two photomultiplier tubes (PMTs) operating in the photon-counting mode with time strobing of the signal, which provides the altitude resolution from 37.5 to 150 m [19]. To suppress active backscattering interference from the near lidar zone (up to 3 km), electro-optical shutters (EOSs) based on a potassium dideuterium phosphate (DKDP) crystal are installed in front of the PMTs. The use of EOSs allows the PMT characteristics to be maintained linearly even during lidar operation in the daytime with the maximum energy of the sensing pulse.

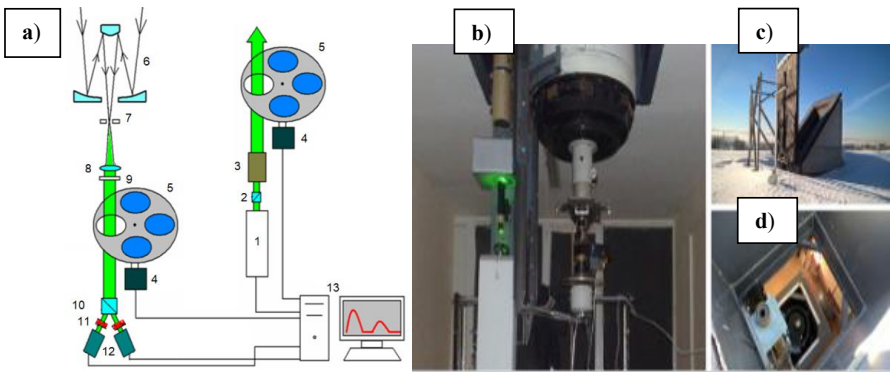

Figure 1. HAMPL: (**a**) block diagram: 1—laser; 2—Glan–Taylor prism; 3—collimator; 4—stepper motor; 5—polarization transformation unit; 6—Cassegrain telescope; 7—field stop; 8—lens; 9—interference filter; 10—Wollaston prism; 11—PMTs; 12—EOSs; 13—computer-based data recording and displaying equipment [19]; (**b**) view of the receiving and transmitting part; (**c**) view on the roof of the building; (**d**) view from the roof of the building.

During each sensing cycle, pulses of radiation with four different polarization states (three linear and one circular) were sent to the atmosphere one by one. The polarization state of backscattered radiation described by the Stokes vector was determined for each pulse. Thus, 16 intensity vertical profiles, from which BSPM elements were calculated, were measured in each sensing cycle. The HAMPL provided the registration of lidar returns from HLC in the parallel accumulation regime of 16 arrays of single-electron pulses. This regime allows the intensity of all mentioned intensities to be estimated with the same error. During sensing in the parallel accumulation regime, the polarization elements in the transmitting and receiving systems of the lidar are constantly changing, as a result of which, at a repetition rate of 10 Hz sensing pulses, the minimum time of a complete measurement cycle for determining all BSPM elements is 2 seconds [18, 19]. Lidar signal processing is based on the application of the laser sensing equation (LSE). In vector form, it is represented as follows [16]:

$$P(z)s(z) = \frac{1}{2}cW_0\frac{A}{z^2}G(z)M_\pi s_o \exp \left\{-2\int_0^{z_0}\varepsilon(z',\theta,\varphi)dz'\right\} \quad (1)$$

Where $P(z)$ and $s(z)$ are the power and the normalized Stokes vector parameter of radiation incident on the input of the lidar receiving system from the scattering volume located on the sensing path at a distance z from the source, respectively; c is the speed of light in the medium; $W_0 = P_0\Delta t$ is the pulse energy of the lidar transmitter (P_0 and Δt are the power and duration of the laser pulse, respectively); A is the effective area of the receiving antenna; $G(z)$ is the geometric factor (when sensing high-level clouds, $G(z)$ is usually equals to 1); $\boldsymbol{M}_\pi(z)$ is the normalized BSPM of the scattering volume; s_0 is the normalized Stokes vector-parameter of sensing radiation; $\varepsilon(z',\theta,\varphi)$ is the attenuation coefficient; θ and φ are the polar and azimuthal angles, respectively. Note that the value of P(z) in (1) is corrected for additive interference caused by solar radiation scattered by HLCs. The intensity of this radiation is measured for each laser pulse sent into the atmosphere and, accordingly, the amount of scattered solar radiation entering the lidar receiving system can be subtracted from the total flow.

As mentioned above, information about the optical and microphysical characteristics of a cloud is available from lidar experiments, is contained in the MORS. From a mathematical point of view, it is an operator for converting the Stokes vector-parameter describing the polarization state of sensing radiation into the Stokes vector-parameter of backscattered radiation received by the lidar. Wherein, the polarization state of scattered radiation depends on the scattering volume properties, namely, on the concentration and composition of scattering particles, on their size, shape and spatial orientation. In other words, the BSPM physically contains information about the microstructure of the cloud.

The procedure for determining the noise level in the lidar receiving channel is relatively simple and, at the same time, original. For this purpose, the time interval between two consecutive sensing laser pulses is used. Since HLCs in the middle latitudes are located at altitudes from 5 to 10–12 km, it can be assumed that the backscatter signal from such clouds lasts no more than 100 microseconds from the moment the probing pulse is sent. Therefore, in the time interval from 100 to 1000 microseconds, the lidar receiving system will register a background radiation flux, which in the daytime is mainly due to the brightness of the daytime sky and the stream of scattered solar radiation entering the lidar receiving system.

The NR TSU HAMPL is in the southern part of Tomsk (56°26′ N 84°58′ E), about 0.5 km from the bank of the Tom' River. Measurements are performed in the absence of low clouds and precipitation. The duration of one series of lidar measurements is usually 16 minutes and 40 seconds. The description of the distributions of the number of lidar measurements and the number of cases of HLC registration in them by year and season was previously published [18, 19]. In the present article, the data from lidar experiments performed in 2020–2023 are considered. During this time period, HLCs were recorded during 40% of the lidar measurement series. To evaluate the meteorological conditions at the altitudes of the examined clouds, we relied on data from the ERA5 reanalysis provided by the European Centre for Medium-range Weather Forecasts [19]. The most reliable source of data on the vertical profiles of meteorological parameters is radiosonde observations, although the nearest stations to Tomsk where radiosonde launches are performed regularly are approximately 200–

230 km away (Kolpashevo and Novosibirsk). Although the meteorological conditions at the altitudes of cloud formation in the upper atmosphere are usually similar according to these data, the ERA5 reanalysis provides a higher temporal resolution (1 hour compared to 12 hours). With a high spatial resolution (30 × 30 km), the ERA5 reanalysis provides vertical profiles of the meteorological parameters and Tomsk coordinates [20]. As initial data for the ERA5, measurements from various sources around the globe are used: satellite radiometers, ground-based, ship-based and aircraft weather stations, weather buoys, balloon-borne sensors, and ground-based radars [21]. At the HLC formation altitudes, the vertical resolution of the ERA5 data is 25–50 hPa, which is approximately equivalent to 0.5–1 km. To evaluate the meteorological situation at the formation altitudes of the examined clouds, the altitudes of their boundaries are determined based on the lidar measurement data, for which the corresponding reanalysis data are then adjusted by coordinates, date, time, and altitude.

3. Results

To test the hypothesis that the signals measured during lidar experiments are independent of the zenith and azimuth angles of the Sun's position, these angles were calculated using a similar method as described in [22]. The input parameters for the calculations included the coordinates and time zone of the observation location, as well as the specific date and time. There is a known issue in treating azimuthal and zenith angle values when they approach 360 degrees – a discontinuity, which can cause errors in program calculations due to the large numerical difference between angles that are essentially adjacent. For example, the angles 359° and 1° are mathematically close, but their direct numerical representation introduces a sharp transition, leading to inconsistencies when performing trigonometric calculations. We converted the angular values into a continuous distribution by calculating their sine and cosine components to ensure that angles, which are next to each other on a circular scale, are handled consistently by the algorithms. Four continuous variables from the sine and cosine of both the azimuthal and zenith angles were computed and then used in the analysis.

In the previous study [17], the relationship between the HLC BSPM elements and altitude was investigated, with results showing no significant correlation. Based on these results, in this study, for each set of lidar measurements, the median values from the experimental sample were used as the values for the BSPM elements. The article [17] also demonstrates that only the elements on the matrix main diagonal (m_{22}, m_{33}, and m_{44}) have a specific dependence on meteorological variables.

As previously mentioned, a dataset used in this research has been generated from the median values of BSPM elements and their associated date, time, coordinates, and altitude values for meteorological parameters based on the ERA5 data [23]. This dataset was then enhanced by including the sine and cosine values of the Sun's azimuth and zenith angles. After that, the lidar data were split into training and validation sets, with the training set containing only meteorological data and the validation set incorporating solar position data. The results of the trained models were then evaluated and compared. Random Forest (RF) models were used, including a version with data preprocessing using principal component analysis (RF+PCA). The validation sample that was held out used to assess the accuracy of the models' forecasts for HLC characteristics was generated from data covering the period from February 15, 2020, to September 22, 2023 (65 observations). This validation set was not used during the training phase, allowing for an unbiased assessment of the model's ability.

After training the ML algorithms, the validation dataset was used to assess the accuracy of the models in predicting the BSPM elements. In the process of choosing the optimal algorithms for predicting the values of the BSPM elements, all possible variants of the number of components in the PCA method were investigated.

The performance of the models trained on two datasets – one including solar data and one without them – was compared using a metric in the form of a mean squared error (2). This metric was calculated between the values predicted by the algorithm and the actual experimental data. The results are presented in **Table 1**. RF stands for the random forest algorithm, while PCA represents the data that has been preprocessed using the principal component analysis (the number of components used is indicated in parentheses).

$$MSE = \frac{1}{N} \sum_{i=1}^{N} (y_{true}^{i} - y_{predict}^{i})^2 \quad (2)$$

The best results in terms of the predictive ability of the algorithms were obtained from the data processed using PCA with the number of components equal to 9 and 15. The number of possible components varies from 1, which is necessary for the presence of at least one training feature, to the total number of available features, which is 65, among which 5 meteorological values were collected at 13 different altitudes.

Specifically, for element m_{22}, the RF+PCA method with 15 components showed an improvement of 2.36%, which is a positive result. However, for element m_{33}, a deterioration of 6.17% is observed when using RF+PCA with 15 components, indicating the need for further analysis. The RF+PCA method with 9 components also demonstrated an improvement for element m_{22} of 1.43% and a slight improvement for element m_{33} of 0.44%. For element m_{44}, the results remain close to the initial values, with minor changes, which may indicate the stability of this element when applying different methods.

The "Percentage of improvement" column provides a quantitative description of the correspondence of the HLC BSPM elements predicted by machine learning methods obtained during lidar measurements using the two mentioned data sets. As can be observed from **Table 1**, there has been no significant and consistent improvement in the performance of any of the algorithm types. There are minor differences in the algorithm's output when comparing results without the use of the Sun's zenith and azimuth angles compared to those with them. Although the estimated improvements are up to several percent, the differences in the results obtained using both methods are small (0.0001–0.001). The change in predictive capability is within a range of no more than 7%. This indicates that the addition of data regarding the position of the Sun has a random effect on the behavior of the algorithms, and none of the presented algorithms was able to identify a stable dependency for any element or demonstrate more confident results. Higher performance metrics for algorithms using the principal component method may suggest that the application of this preprocessing method introduces additional randomness, which can lead to slight improvements. However, these improvements are driven by random factors and are not significant. Therefore, even significant differences in the percentage of improvement among the three machine learning techniques used, which amount to a few percent, are not explainable from the perspective of atmospheric optics. The results obtained suggest that the inclusion of the Sun's zenith and azimuth angle in the experimental dataset used to train the machine learning models does not significantly impact their predictive ability when searching for correlations between HLC BSPM elements and meteorological parameters.

Table 1. The results of a comparative analysis of the algorithms.

Method	The Predicted HLC BSPM Element	The MSE Value Obtained without Using the Angles of the Sun's Position	The MSE Value Obtained with Using the Angles of the Sun's Position	Difference	Improvement Percentage, %
RF	m_{22}	0.03623	0.03635	–0.00012	–0.33
	m_{33}	0.05577	0.05551	0.00026	0.47
	m_{44}	0.11618	0.11811	–0.00193	–1.66
RF+PCA (15)	m_{22}	0.0292	0.02851	0.00069	2.36
	m_{33}	0.05621	0.05968	–0.00347	–6.17
	m_{44}	0.09536	0.09524	0.00012	0.13
RF+PCA (9)	m_{22}	0.02929	0.02887	0.00042	1.43
	m_{33}	0.06383	0.06355	0.00028	0.44
	m_{44}	0.09547	0.09998	–0.00451	–4.72

It should be noted that the table presents the results of the three most effective models, demonstrating the best predictive performance on data that does not contain information about solar coordinates. Within the framework of this study, various algorithms were also tested, including neural networks, linear regression, and other machine learning methodologies. The analysis showed that the behavior of these algorithms remained unchanged when solar data was added, indicating the absence of a significant improvement in the predictive capability of the models as a result of integrating additional information about solar activity. The inclusion of information about the position of the sun may potentially affect the results of the analysis. Studies show that components based on the principal component method may be sensitive to the presence of additional factors, such as solar activity, which in turn could improve the predictive capability of the model. Such results can be explained by several factors. Firstly, it is possible that solar coordinates do not have a significant impact on the variable under study, indicating their insignificance in this context. Secondly, it is assumed that the model already sufficiently accounts for other factors that may be more critical for prediction. For a deeper understanding of this phenomenon and to assess the impact of solar data on the predictive capability of the models, further research is necessary. It is important to explore the correlation dependencies between solar activity and the target variable, as well as to consider the possibility of applying feature selection methods to identify hidden dependencies. Additionally, it may be worthwhile to use more advanced data processing and analysis methods, such as ensemble methods or deep learning techniques, which may be more sensitive to latent interactions between variables.

4. Conclusions

In the present work, a random forest algorithm is considered to determine the dependence of the HLC BSPM elements determined in the experiments on polarization laser sensing of the atmosphere on the measurement parameters. Previously, meteorological parameters and the Sun's zenith and azimuth were considered as measurement parameters. A hypothesis was formulated and verified about the absence of an effect of the Sun's position on the signals measured in lidar experiments, and, consequently, on the predicted BSPM elements. The results demonstrated that the inclusion of the Sun's angles did not lead to significant or consistent improvements in the prediction of BSPM elements. In several cases, we have observed that algorithms using solar data as an input parameter may experience a degradation in their predictive capabilities. For example, when using the RF + PCA (15) algorithm to predict the m_{33} element, we observed a degradation of 6.47%. At the same time, if the algorithms were to improve their performance, it would not be by more than 1.5%. For element m_{44}, the results remain close to the initial values, with minor changes, which may indicate the stability of this element when applying different methods. The change in predictive capability is within a range of no more than 7%. This indicates that the addition of data regarding the position of the Sun has a random effect on the behavior of the algorithms, and none of the presented algorithms was able to identify a stable dependency for any element or demonstrate more confident results. Higher performance metrics for algorithms using the principal component method may suggest that the application of this preprocessing method introduces additional randomness, which can lead to slight improvements. However, these improvements are driven by random factors and are not significant. Therefore, even significant differences in the percentage of improvement among the three machine learning techniques used, which amount to a few percent, are not explainable from the perspective of atmospheric optics. It was concluded that, in general, there is no significant tendency for the Sun's angles to affect the algorithm's predictive ability. These findings support the initial hypothesis that the Sun's azimuth and zenith angles do not significantly influence the accuracy of lidar-based cloud measurements.

5. Patents

The research was carried out with the support of a grant from the Government of the Russian Federation (Agreement No. 075-15-2025-009 of 28 February 2025) in the part of the potential of using the effect of anisotropic solar radiation scattering on the prediction accuracy of machine learning models for predicting the elements of backscattering phase matrix (BSPM) of HLC was explored. This research was funded by the Russian Science Foundation, Grant No. 24-72-10127 in the part of studying the re-

lationship between the optical, microphysical, and geometric characteristics of high-level clouds with predominantly horizontally oriented ice particles and the meteorological conditions leading to their formation and evolution.

Author Contributions

I.S., O.K., I.B., and M.P. developed the idea of this work. I.S. and I.B. conducted a preliminary analysis and interpretation of lidar and meteorological data. O.K., and M.P. developed a software product using machine learning tools for analyzing meteorological observation data and predicting optical and geometric characteristics of the HLC. I.A. and D.R. programmatically compared two approaches to learning algorithms (with and without solar data) for predicting HLC BSPM elements. E.N. and I.Z. performed experiments on lidar sensing of the atmosphere. I.B., M.P., O.K., and I.S. analyzed the measurement and calculated data. I.B., M.P., O.K., I.S., I.A., and D.R. discussed the results, wrote, and edited the article. All authors have read and agreed to the published version of the manuscript.

Funding

This work was supported by the Government of the Russian Federation grant number 075-15-2025-009 of 28 February 2025 and by the Russian Science Foundation, Grant No. 24-72-10127.

Institutional Review Board Statement

Not applicable.

Informed Consent Statement

Not applicable.

Data Availability Statement

In this study, publicly available meteorological datasets were analyzed. The data can be accessed at the following links: [http://weather.uwyo.edu] and [https://cds.climate.copernicus.eu]. The atmospheric remote sensing data at HAMPL of Tomsk State University presented in this study are available upon request from the corresponding author.

Conflicts of Interest

The authors declare no conflict of interest.

References

[1] Wilson, L., Goh, T.T., Wang, C., 2020. Big Data in Climate Change Research: opportunities and Challenges. In Proceedings of the 2020 International Conference on Intelligent Engineering and Management (ICIEM); London, UK, 17-19 June 2020; Volume 4, pp. 1–14. DOI: https://doi.org/10.1109/ICIEM48762.2020.9160174

[2] Isaksen, I.S.A., Granier, C., Myhre, G., et al., 2009. Atmospheric composition change: Climate–Chemistry interactions. Atmospheric Environment. 43, 5138–5192. DOI: https://doi.org/10.1016/j.atmosenv.2009.08.003

[3] Wilks, D.S., 2006. Statistical Methods in the Atmospheric Sciences, 2nd ed.; Academic Press, International Geophysics Series, USA. 627p.

[4] Lapčák, M., Ovseník, Ľ., Oravec, J., et al., 2022. Investigation of Machine Learning Methods for Prediction of Measured Values of Atmospheric Channel for Hybrid FSO/RF System. Photonics. 9(8), 524. DOI: https://doi.org/10.3390/photonics9080524

[5] Ukkonen, P., 2022. Exploring Pathways to More Accurate Machine Learning Emulation of Atmospheric Radiative Transfer. Journal of Advances in Modeling Earth Systems. 14, e2021MS002875. DOI: https://doi.org/10.1029/2021MS002875

[6] Veerman, M.A., Robert, P., Robin, S., et al., 2021. Predicting atmospheric optical properties for radiative transfer computations using neural networks. Philosophical Transaction A. 379, 20200095. DOI: https://doi.org/10.1098/rsta.2020.0095

[7] Guide on actinometric observations for hydrometeorological stations, 3rd ed.; Gidrometeoizdat: Leningrad, Russia, 1973. (In Russian)

[8] Andrews, E., Ogren, J.A., Bonasoni, P., et al., 2011. Climatology of aerosol radiative properties in the free troposphere. Atmospheric Research. 102(4), 365–393. DOI: https://doi.org/10.1016/j.atmosres.2011.08.017

[9] Abakumova, G.M., Gorbarenko, E.V., 2008. Transparency of the atmosphere in Moscow over the past 50 years and its changes in Russia, LKI Publishing House: Moscow, Russia. (In Russian)

[10] Liepert, B.G., 2002. Observed reductions of surface solar radiation at sites in the United States and worldwide from 1961 to 1990. Geophysical Research Letters. 29(10), Article No. 61. DOI: https://doi.org/10.1029/2002GL014910

[11] Luo, H., Han, Y., Lu, C., et al., 2019. Characteris-

tics of Surface Solar Radiation under Different Air Pollution Conditions over Nanjing, China: Observation and Simulation. Advances in Atmospheric Sciences. 36, 1047–1059. https://link.springer.com/article/10.1007/s00376-019-9010-4

[12] Haverkort, A.J., Uenk, D., Veroude, H., et al., 1991. Relationships between ground cover, intercepted solar radiation, leaf area index and infrared reflectance of potato crops. Potato Research. 34, 113–121. https://link.springer.com/article/10.1007/BF02358105

[13] Feigelson, E.M. (Ed.), 1989. Radiation Properties of Perispheric Clouds; Nauka: Moscow, Russia. (In Russian)

[14] Dmitrieva-Arrago, L.R., Trubina, M.A., Tolstyh, M.A., 2017. Role of Phase Composition of Clouds in Forming High and Low Frequency Radiation. Trudy Gidromettsentra Rossii. 363, 19–34. (In Russian)

[15] Rozenberg, G.V., 1955. Stokes vector parameter (matrix methods for accounting radiation polarization in the ray optics approximation). Uspekhi Fizicheskikh Nauk. 56, 79–110. (In Russian)

[16] Kaul, B.V., 2004. Optical-Location Method of Polarization Studies of Anisotropic Aerosol Media [Doctor's Dissertation]. Physical-Mathematical Sciences: Tomsk, Russia. (In Russian)

[17] Kuchinskaia, O., Penzin, M., Bordulev, I., et al., 2024. Artificial Neural Networks for Determining the Empirical Relationship between Meteorological Parameters and High-Level Cloud Characteristics. Applied Sciences. 14(5), 1782. https://doi.org/10.3390/app14051782

[18] Bryukhanov, I.D., Kuchinskaia, O.I., Ni, E.V., et al., 2024. Optical and Geometrical Characteristics of High-Level Clouds from the 2009–2023 Data on Laser Polarization Sensing in Tomsk. Atmospheric and Oceanic Optics. 37, 343–351. https://link.springer.com/article/10.1134/S1024856024700441

[19] Kuchinskaia, O., Bryukhanov, I., Penzin, M., et al., 2023. ERA5 Reanalysis for the Data Interpretation on Polarization Laser Sensing of High-Level Clouds, Remote Sensing. 15(1), 109. DOI: https://doi.org/10.3390/rs15010109

[20] ECMWF Reanalysis v5 (ERA5). Available from: https://www.ecmwf.int/en/forecasts/dataset/ecmwf-reanalysis-v5 (cited 19 September 2024).

[21] ECMWF Confluence Wiki. ERA5: data documentation. Available from: https://confluence.ecmwf.int/display/CKB/ERA5%3A+data+documentation#ERA5:datadocumentation-Introduction (cited 19 November 2024).

[22] Rizvi, A.A., Addoweesh, K., El-Leathy, A., et al., 2014. Sun position algorithm for sun tracking applications. In Proceedings of the IECON 2014 – 40th Annual Conference of the IEEE Industrial Electronics Society. Dallas, TX, USA. 5595–5598.

[23] Copernicus Climate Data Store. Available from: https://cds.climate.copernicus.eu (cited 19 November 2024).